

# Dynamical friction on hot bodies in opaque, gaseous media

Frédéric S. Masset <sup>\*</sup> and David A. Velasco Romero

*Instituto de Ciencias Físicas, Universidad Nacional Autónoma de México, Av. Universidad s/n, 62210 Cuernavaca, Mor., Mexico*

Accepted Nov. 17, 2016; Received Nov. 1, 2016; in original form Sep. 10, 2016

## ABSTRACT

We consider the gravitational force exerted on a point-like perturber of mass  $M$  traveling within a uniform gaseous, opaque medium at constant velocity  $\mathbf{V}$ . The perturber irradiates the surrounding gas with luminosity  $L$ . The diffusion of the heat released is modelled with a uniform thermal diffusivity  $\chi$ . Using linear perturbation theory, we show that the force exerted by the perturbed gas on the perturber differs from the force without radiation (or standard dynamical friction). Hot, underdense gas trails the mass, which gives rise to a new force component, the heating force, with direction  $+\mathbf{V}$ , thus opposed to the standard dynamical friction. In the limit of low Mach numbers, the heating force has expression  $F_{\text{heat}} = \gamma(\gamma - 1)GML/(2\chi c_s^2)$ ,  $c_s$  being the sound speed and  $\gamma$  the ratio of specific heats. In the limit of large Mach numbers,  $F_{\text{heat}} = (\gamma - 1)GML/(\chi V^2)f(r_{\text{min}}V/4\chi)$ , where  $f$  is a function that diverges logarithmically as  $r_{\text{min}}$  tends to zero. Remarkably, the force in the low Mach number limit does not depend on the velocity. The equilibrium speed, when it exists, is set by the cancellation of the standard dynamical friction and heating force. In the low Mach number limit, it scales with the luminosity to mass ratio of the perturber. Using the above results suggests that Mars- to Earth-sized planetary embryos heated by accretion in a gaseous protoplanetary disc should have eccentricities and inclinations that amount to a sizeable fraction of the disc’s aspect ratio, for conditions thought to prevail at a few astronomical units.

**Key words:** hydrodynamics – gravitation – planet-disc interactions

## 1 INTRODUCTION

A massive perturber moving across a medium triggers a disturbance in this medium, by gravity. Dynamical friction is the back reaction of this disturbance on the perturber itself. It is directed against the motion of the perturber, which it tends to slow down. Initially worked out for collisionless media by Chandrasekhar (1943), it was subsequently studied in gaseous media (Rephaeli & Salpeter 1980; Ostriker 1999). It has been initially suggested that in the subsonic regime in gaseous media there would be no net force exerted on the perturber (Rephaeli & Salpeter 1980), owing to the symmetry of the perturbed density field with respect to the perturber, in steady state. However, Ostriker (1999) showed that a time-dependent analysis is required to correctly evaluate the net force in the subsonic regime: the disturbance is at all times contained within a sonic sphere centred on the initial location of the perturber, which induces asymmetries in the far-field with respect to the actual position of the perturber. These asymmetries ultimately yield a constant net force, which increases with the Mach number, and scales with the velocity of the perturber in

the limit of a low Mach number. This analysis, performed in the framework of linear perturbation theory, was subsequently corroborated by the non-linear numerical simulations of Sánchez-Salcedo & Brandenburg (1999).

In the supersonic regime, the force is inversely proportional to the square of the velocity in the limit of a large Mach number. Also, in this regime, the force scales with the logarithm of the ratio of the maximal to minimal distance over which the medium is perturbed. The divergence of this quantity at large scale is suppressed if the perturber moves in a slab or protoplanetary disc (Papaloizou 2002; Muto et al. 2011; Cantó et al. 2013). The minimal distance has been found to be of the order of the gravitational radius  $GM/V^2$  by Cantó et al. (2011), who performed non-linear calculations in the ballistic approximation.

Dynamical friction can be used to study some aspects of planet-disc tidal interactions (Papaloizou 2002; Muto et al. 2011). While the time evolution of orbital elements of low-eccentricity objects must be obtained by a resonant torque calculation, the behaviour of objects with an eccentricity larger than the disc’s aspect ratio can be obtained through a dynamical friction calculation. In this regime indeed, the disc’s response becomes local and the Keplerian shear can be neglected.

\* E-mail: masset@icf.unam.mx

It has been recently shown that the modification of the disc's structure by a hot protoplanet that irradiates its immediate surroundings can significantly alter the tidal force from the disc, with a sizeable impact on planetary migration (Benitez-Llambay et al. 2015). This comes from the fact that the force arising from the disturbance due to the heat release has the same order of magnitude as the force due to the disturbance induced by the planet's gravity. Motivated by the serendipitous coincidence between the order of magnitude of these two forces, we investigate here the impact of heat release in the simpler context of dynamical friction, using linear perturbation theory. We lay down our equations in section 2, and work out the force arising from heat release in the limits of low Mach numbers (section 3) and large Mach numbers (section 4). We then discuss the behaviour of a perturber subjected to the sum of the heating force and standard dynamical friction in section 5. We finally discuss the case of planetary embryos and protoplanets heated by accretion, embedded in opaque protoplanetary discs, in section 6, and sum up our findings in section 7.

## 2 GOVERNING EQUATIONS

We consider the linearised equations for the perturbations of density  $\rho$ , energy density  $e$  and velocity  $\mathbf{v}$  of an ideal gas with uniform unperturbed density  $\rho_0$ , energy density  $e_0$  and velocity  $\mathbf{v}_0$ , subjected to the gravity of a point-like mass  $M$ , located at the position  $\mathbf{r}_0$ , and releasing energy at the constant rate  $L$ :

$$\partial_t \rho + \mathbf{v}_0 \cdot \nabla \rho + \rho_0 \nabla \cdot \mathbf{v} = 0 \quad (1)$$

$$\partial_t \mathbf{v} + (\mathbf{v}_0 \cdot \nabla) \mathbf{v} + \frac{\nabla p}{\rho_0} = -\nabla \Phi \quad (2)$$

$$\partial_t e + \mathbf{v}_0 \cdot \nabla e + \gamma e_0 \nabla \cdot \mathbf{v} + \frac{e_0}{\rho_0} \chi \Delta \rho - \chi \Delta e = L \delta(\mathbf{r} - \mathbf{r}_0), \quad (3)$$

where

$$\Phi = -\frac{GM}{|\mathbf{r} - \mathbf{r}_0|} \quad (4)$$

is the gravitational potential of the mass,  $\chi$  is the thermal diffusivity of the gas,  $\gamma$  is the ratio of specific heats and  $p$  is the pressure. The last two terms of the left hand side of Eq. (3) come from the linearisation of the divergence of the energy flux density  $\mathbf{q}$  arising from heat conduction and given by Fourier's law:

$$\mathbf{q} = -c_v \rho_0 \chi \nabla T, \quad (5)$$

where  $c_v$  is the specific heat at constant volume and where the temperature  $T$  is given by  $T = (e_0 + e)/[c_v(\rho_0 + \rho)]$ . The perturbations of energy density and pressure are related by:

$$p = (\gamma - 1)e \quad (6)$$

and a similar relationship holds for the unperturbed quantities. We denote  $c_s$  the adiabatic sound speed:

$$c_s = \sqrt{\frac{\gamma(\gamma - 1)e_0}{\rho_0}}. \quad (7)$$

Assuming the perturber is introduced at  $t = 0$ , we write  $\rho_{M,L}(\mathbf{r}, t)$  the solution of the linear system of Eqs. (1)-(3),

and  $\mathbf{F}_{M,L}(t)$  the force exerted by the gas on the perturber:

$$\mathbf{F}_{M,L}(t) = GM \iiint \frac{\rho_{M,L}(\mathbf{r}, t)(\mathbf{r} - \mathbf{r}_0)}{|\mathbf{r} - \mathbf{r}_0|^3} d^3 \mathbf{r}. \quad (8)$$

We have:

$$\rho_{M,L}(\mathbf{r}, t) = \rho_{M,0}(\mathbf{r}, t) + \rho_{0,L}(\mathbf{r}, t), \quad (9)$$

which reads that the density perturbation  $\rho_{M,L}$  due to a massive and luminous perturber of mass  $M$  and luminosity  $L$  is the sum of the density perturbations respectively due to a massive, non-luminous perturber ( $\rho_{M,0}$ ) and to a massless, luminous perturber ( $\rho_{0,L}$ ). We write:

$$\mathbf{F}_{M,L}(t) = \mathbf{F}_{\text{DF}}(t) + \mathbf{F}_{\text{heat}}(t), \quad (10)$$

where  $\mathbf{F}_{\text{DF}}(t)$  and  $\mathbf{F}_{\text{heat}}(t)$  are the forces arising respectively from the density distributions  $\rho_{M,0}(\mathbf{r}, t)$  and  $\rho_{0,L}(\mathbf{r}, t)$ . The expression of  $\mathbf{F}_{\text{DF}}(t)$ , which we call hereafter the standard dynamical friction, has been worked out by Ostriker (1999) for a perturber in an adiabatic gas. We seek here an expression for  $\mathbf{F}_{\text{heat}}(t)$  in steady state, which we call the heating force. In sections 3 and 4 below we work out the heating force alone, respectively in the limits of low and large Mach numbers. Subsequently we give an estimate of the total force in section 5.

## 3 HEATING FORCE IN THE LIMIT OF A LOW MACH NUMBER

### 3.1 Perturbation of density field

We place ourselves in the perturber frame and set  $\mathbf{v}_0 = -\mathbf{V}$ ,  $\mathbf{r}_0 = \mathbf{0}$  in Eqs. (1)-(3), where  $\mathbf{V}$  is the velocity of the perturber with respect to the gas. We use a Cartesian frame  $(x, y, z)$  such that  $\mathbf{V} = V\hat{\mathbf{z}}$ , and we assume a steady state. Eqs. (1)-(3) can be recast as:

$$-V\partial_z \rho + \rho_0 \nabla \cdot \mathbf{v} = 0 \quad (11)$$

$$-V\partial_z v_j + \frac{\partial_j p}{\rho_0} = 0 \quad j = 1, 2, 3 \quad (12)$$

$$-V\partial_z p + \gamma p_0 \nabla \cdot \mathbf{v} + \frac{c_s^2}{\gamma} \chi \Delta \rho - \chi \Delta p = (\gamma - 1)L\delta(\mathbf{r}) \quad (13)$$

We denote with a tilde the three-dimensional Fourier transform, adopting the following conventions of sign and normalisation:

$$\begin{aligned} \tilde{\rho}(\mathbf{k}) &= \iiint \rho(\mathbf{r}) e^{-i\mathbf{k}\cdot\mathbf{r}} d^3 \mathbf{r} \\ \rho(\mathbf{r}) &= \frac{1}{(2\pi)^3} \iiint \tilde{\rho}(\mathbf{k}) e^{i\mathbf{k}\cdot\mathbf{r}} d^3 \mathbf{k} \end{aligned} \quad (14)$$

Eq. (12) becomes:

$$Vk_z \tilde{v}_j = k_j \frac{\tilde{p}}{\rho_0}. \quad (15)$$

Multiplying Eq. (15) by  $k_j$  and summing on  $j$ , then using Eq. (11), we obtain the relation:

$$k^2 \tilde{p} = V^2 k_z^2 \tilde{\rho}, \quad (16)$$

where  $k^2 = k_x^2 + k_y^2 + k_z^2$ . Using Eqs. (16) and (11) to substitute respectively the pressure and the divergence of velocity in Eq. (13), we obtain:

$$\tilde{\rho}(k_x, k_y, k_z) = \frac{(\gamma - 1)L}{\chi \left( k_z^2 V^2 - \frac{c_s^2}{\gamma} k^2 \right) + i \left( c_s^2 - \frac{k_z^2 V^2}{k^2} \right) k_z V}.$$

(17)

In the limit  $(V/c_s)^2 \ll 1/\gamma$ ,  $\tilde{\rho}$  can be approximated by

$$\tilde{\rho}(k_x, k_y, k_z) = -\frac{\gamma(\gamma-1)L/c_s^2}{\chi k^2 - i\gamma k_z V}. \quad (18)$$

We introduce the function:

$$R(\mathbf{r}) = \rho(\mathbf{r})e^{z\gamma V/2\chi}, \quad (19)$$

which has the following Fourier transform:

$$\begin{aligned} \tilde{R}(k_x, k_y, k_z) &= \tilde{\rho}\left(k_x, k_y, k_z + i\frac{\gamma V}{2\chi}\right) \\ &= -\frac{\gamma(\gamma-1)L/c_s^2}{\chi k^2 + \frac{\gamma^2 V^2}{4\chi}}. \end{aligned} \quad (20)$$

The inverse Fourier transform of Eq. (20) yields

$$R(\mathbf{r}) = -\frac{\gamma(\gamma-1)L e^{-r\gamma|V|/2\chi}}{4\pi\chi c_s^2 r}, \quad (21)$$

and thus

$$\rho(\mathbf{r}) = -\frac{\gamma(\gamma-1)L}{4\pi\chi c_s^2 r} e^{-z\gamma V/2\chi} e^{-r\gamma|V|/2\chi}. \quad (22)$$

On the  $z$ -axis ( $r = |z|$ ), in the upstream flow ( $z \text{ sign}(V) > 0$ ), the density perturbation follows the law:

$$\rho(0, 0, z) = -\frac{\gamma(\gamma-1)L}{4\pi\chi c_s^2 r} e^{-|z|/\lambda}, \quad (23)$$

where the cut-off distance

$$\lambda = \chi/\gamma|V| \quad (24)$$

is set by the competition between diffusion and advection and represents the typical distance over which the heat can diffuse against the headwind. Remarkably, the density perturbation on the  $z$ -axis in the downstream flow ( $z \text{ sign}(V) < 0$ ) follows a law that is indistinguishable from the law without headwind:

$$\rho(0, 0, z) = -\frac{\gamma(\gamma-1)L}{4\pi\chi c_s^2 r}. \quad (25)$$

We will hereafter refer to  $\lambda$  as the cut-off distance or, more informally, as the size of the hot plume, since it represents the typical size of the perturbed region.

### 3.2 Force expression

We substitute Eq. (22) in (8), which we express using spherical coordinates. Without loss of generality, we assume here  $V > 0$ . This yields:

$$F_{\text{heat}} = -\frac{\gamma(\gamma-1)GML}{2\chi c_s^2} I, \quad (26)$$

where  $I$  is given by:

$$I = \int_0^\infty \int_0^\pi \frac{1}{r} \cos\theta e^{r/2\lambda(-1-\cos\theta)} \sin\theta d\theta dr \quad (27)$$

We perform the change of variable  $u = \cos\theta$  and integrate by parts in  $u$ , which yields

$$I = -\int_0^\infty \frac{1+e^{-2r'}}{r'^2} - \frac{1-e^{-2r'}}{r'^3} dr', \quad (28)$$

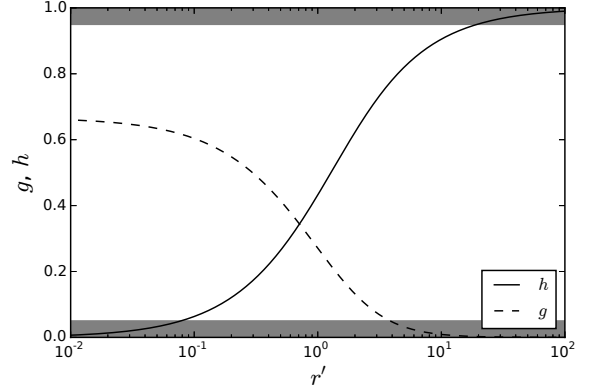


**Figure 1.** Graphs of functions  $g$  (dashed line) and  $h$  (solid line), respectively given by Eqs. (31) and (32). The greyed areas represent the innermost and outermost five percent contributions, which are respectively obtained for  $r' = 0.078$  and  $r' = 19.5$ .

with  $r' = r/2\lambda$ . We have:

$$I = -\left. \frac{1-2r' - e^{-2r'}}{2r'^2} \right|_0^\infty = -1. \quad (29)$$

If we now relax the assumption  $V > 0$ , then using the symmetry  $V \rightarrow -V$ ,  $\rho(x, y, z) \rightarrow \rho(x, y, -z)$ , we finally express the heating force, in the regime of low Mach numbers, as:

$$F_{\text{heat}} = \frac{\gamma(\gamma-1)GML}{2\chi c_s^2} \text{sign}(V). \quad (30)$$

It is therefore directed along the direction of motion, and has a magnitude independent of  $V$  and  $\rho_0$ . We show in Fig. 1 the integrand of Eq. (28):

$$g(r') = \frac{1+e^{-2r'}}{r'^2} - \frac{1-e^{-2r'}}{r'^3} \quad (31)$$

and its integral that vanishes for  $r' \rightarrow 0$ :

$$h(r') = \frac{1-2r' - e^{-2r'}}{2r'^2} + 1. \quad (32)$$

The former shows the contribution of spherical shells to the net force and the latter shows the cumulative contribution of all material within radius  $r$  (in units of  $2\lambda$ ). This shows that approximately 40 % of the force arises from the sphere  $r < 2\lambda$ .

### 3.3 Condition for linearity

The assumption that the density perturbation can be given by a linear analysis breaks down when  $\rho$ , given by Eq. (22), has a value comparable to  $\rho_0$ . This happens for  $r < r_{\text{NL}}^{\text{heat}}$ , with

$$r_{\text{NL}}^{\text{heat}} = \frac{\gamma(\gamma-1)L}{4\pi\chi c_s^2 \rho_0}. \quad (33)$$

As long as this radius is small compared to the cut-off distance (which is the characteristic length scale over which the force is produced), Eq. (26) provides a correct value of the heating force. The condition for linearity can therefore be written as:

$$L \ll \frac{4\pi\chi^2 c_s^2 \rho_0}{\gamma^2(\gamma-1)|V|}. \quad (34)$$

Introducing the critical luminosity

$$L_c = \frac{4\pi}{\gamma^2(\gamma-1)} \chi^2 c_s \rho_0, \quad (35)$$

this condition can be recast as:

$$L \ll \frac{L_c}{\mathcal{M}}, \quad (36)$$

where  $\mathcal{M}$  is the Mach number.

### 3.4 Response time

The time for the heating force to develop corresponds to the time it takes to establish the hot, underdense plume. This, in order of magnitude, is also the time it takes for the heat to diffuse over a length scale  $2\lambda$ , which is:

$$\tau \sim \frac{(2\lambda)^2}{4\chi} = \frac{\chi}{\gamma^2 V^2}. \quad (37)$$

We use  $2\lambda$  in this expression since this roughly corresponds to length scale within which half of the heating force arises. We note that  $\tau \rightarrow \infty$  when  $V \rightarrow 0$ . In the special case  $V = 0$ , no heating force ever appears on the perturber, for symmetry reasons. This is a singular case, however: as soon as the perturber has a finite velocity, however small, the heating force eventually develops along the direction of motion.

## 4 HEATING FORCE IN THE LIMIT OF A LARGE MACH NUMBER

In this section we place ourselves in the frame at rest with the gas. For the sake of definiteness we assume  $V > 0$ , and we assume that at the instant at which we evaluate the force, the perturber is at  $z = 0$ . The perturber deposits an amount of energy  $Ldz/V$  in each elementary interval  $[z, z+dz]$ , over the whole negative  $z$ -axis. We firstly evaluate the force due to the disc's response to a singular release of energy at a given value of  $z$ , then we integrate over  $z$  to get the force arising from the perturbation due to an energy release over all the previous positions of the perturber. The time elapsed between the passage of the perturber at a position  $z$  and the time at which it reaches the origin is  $t = |z|/V \ll |z|/c$ . We are therefore interested, when evaluating the force at a distance  $r$  and a time  $t$  after a singular energy release, in the case  $r \gg ct$ .

### 4.1 Force arising from a singular energy deposition

The perturbed density has at any time spherical symmetry about the point of release. By virtue of Gauss's theorem, it suffices to know the variation of the mass enclosed in the sphere centred on the point of release and containing the point where the force is to be evaluated. Here we assume the release to occur at the origin and at  $t = 0$ , and we seek the variation of mass  $\Delta M(r, t)$ . This is tantamount to solving Eqs. (1) to (3) with  $\mathbf{v}_0 = \mathbf{0}$ ,  $L = E\delta(t)$  and  $M = 0$ ,  $E$  being the amount of energy released. Denoting with a bar the space and time Fourier transform:

$$\bar{e}(\mathbf{k}, \omega) = \iiint e(\mathbf{r}, t) e^{-i(\mathbf{k}\cdot\mathbf{r} - \omega t)} d^3\mathbf{r} dt, \quad (38)$$

Eq. (2) yields:

$$\omega \bar{v}_j = k_j \frac{\bar{p}}{\rho_0}. \quad (39)$$

Multiplying Eq. (39) by  $k_j$  and summing on  $j$ , we obtain:

$$\bar{\rho} = \frac{(\gamma-1)k^2}{\omega^2} \bar{e}. \quad (40)$$

Using this relation, we can infer from Eqs. (1) and (3):

$$\bar{e} = \frac{E}{\chi k^2 \left(1 - \frac{k^2 c_s^2}{\gamma \omega^2}\right) + i \left(\frac{c_s^2 k^2}{\omega} - \omega\right)}. \quad (41)$$

Since we are interested in the response at  $r \gg ct$ , the Fourier components that contribute to the response fulfil  $kc_s \ll \omega$ , hence:

$$\bar{e} \approx \frac{E}{\chi k^2 - i\omega}. \quad (42)$$

This corresponds to the solution of the simple diffusion equation

$$\partial_t e - \chi \Delta e = E\delta(t)\delta(\mathbf{r}), \quad (43)$$

which is:

$$e(r, t) = \frac{E}{8\pi^{3/2}(\chi t)^{3/2}} e^{-r^2/4\chi t}. \quad (44)$$

This implies, using Eq. (6) and Eq. (2) with  $\mathbf{v}_0 = 0$  and  $\Phi = 0$ :

$$\partial_t v = \frac{(\gamma-1)Er}{16\rho_0\pi^{3/2}(\chi t)^{5/2}} e^{-r^2/4\chi t}, \quad (45)$$

and upon integration from 0 to  $t$ :

$$v(t) = \int_0^t \partial_t v dt = \frac{(\gamma-1)Er^{-2}}{2\rho_0\pi^{3/2}\chi} \Gamma\left(\frac{3}{2}, \frac{r^2}{4\chi t}\right), \quad (46)$$

where  $\Gamma$  is the upper incomplete gamma function. The mass variation in the sphere of radius  $r$  centred on the release point is obtained by another integration:

$$\begin{aligned} \Delta M(r, t) &= - \int_0^t 4\pi r^2 \rho_0 v(t) dt \\ &= - \frac{2(\gamma-1)E}{\sqrt{\pi}\chi} \int_0^t \Gamma\left(\frac{3}{2}, \frac{r^2}{4\chi t}\right) dt \\ &= - \frac{(\gamma-1)Er^2}{2\sqrt{\pi}\chi^2} \mu\left(\frac{r}{\sqrt{4\chi t}}\right) \end{aligned} \quad (47)$$

where the function  $\mu$  is defined by:

$$\mu(u) = u \exp(-u^2) + \frac{\sqrt{\pi}}{2} (u^{-2} - 2) \operatorname{erfc}(u). \quad (48)$$

Finally, the force arising from this disturbance has the magnitude

$$F(r, t) = - \frac{GM\Delta M(r, t)}{r^2} = \frac{(\gamma-1)GME}{2\sqrt{\pi}\chi^2} \mu\left(\frac{r}{\sqrt{4\chi t}}\right) \quad (49)$$

and is directed opposite the point of release. Fig. 2 shows the graph of  $\mu(u)$  and  $\mu(u^{-1/2})$  which can respectively be seen as the normalised force as a function of  $r$ , in units of  $r_{\text{diff}} = \sqrt{4\chi t}$ , and as the normalised force as a function of  $t$ , in units of  $t_{\text{diff}} = r^2/4\chi$ . A sharp cut-off of the force is found for  $t < t_{\text{diff}}$  (or, equivalently, for  $r > r_{\text{diff}}$ ). The time scale  $t_{\text{diff}}$  is indeed the time it takes for the disturbance created by the energy release to reach the radius  $r$ .

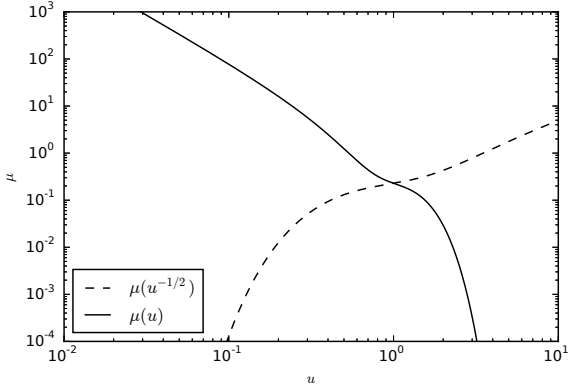


**Figure 2.** Graphs of the functions  $u \mapsto \mu(u)$  (solid line) and  $u \mapsto \mu(u^{-1/2})$  (dashed line).

#### 4.2 Net heating force

We can now complete the procedure outlined at the beginning of section 4 by integrating the force expression of Eq. (49), substituting  $E$  with  $Ldz/V$  and  $t$  with  $r/V$ . In the integral  $r$  represents  $-z$ , where  $z$  runs through the whole set of positions previously occupied by the perturber. We do not integrate all the way to  $r = 0$  however, but rather introduce a minimal radius of integration  $r_{\min}$ , the physical meaning of which will be specified later, as the force integral is found to diverge as  $r_{\min}$  tends to zero. Since the force arising from each elementary release is directed in the direction opposite to the release, as shown in section 4.1, and since the perturber has released energy over the negative  $z$ -axis, the net force is positive. It has the expression:

$$\begin{aligned} F_{\text{heat}} &= - \int_{r_{\min}}^{\infty} \frac{GM\Delta M(r, r/V)}{r^2} dr \\ &= \frac{(\gamma - 1)GML}{2\sqrt{\pi}V\chi^2} \int_{r_{\min}}^{\infty} \mu\left(\frac{rV}{4\chi}\right) dr \\ &= \frac{2(\gamma - 1)GML}{\sqrt{\pi}\chi V^2} f\left(\frac{r_{\min}V}{4\chi}\right), \end{aligned} \quad (50)$$

where  $f$  is given by:

$$f(\epsilon) = \int_{\epsilon}^{\infty} \mu(\sqrt{u}) du. \quad (51)$$

Since  $\mu(\sqrt{u}) \propto 1/u$  when  $u$  tends to zero,  $f$  diverges logarithmically as  $\epsilon$  tends to zero. After some cumbersome manipulations, we can give an equivalent of  $f(\epsilon)$  in the limit  $\epsilon \rightarrow 0$ :

$$f(\epsilon) \approx \frac{\sqrt{\pi}}{2} (-\gamma - 2 \log 2 - \log \epsilon), \quad (52)$$

where, in this expression only,  $\gamma \approx 0.577$  represents the Euler-Mascheroni constant. Note that Eq. (52) is an approximate expression valid only when  $\epsilon \ll 1$ , and that  $f(\epsilon)$  is positive for any value of  $\epsilon$ , since the integrand of the right hand side of Eq. (51) is positive. Fig. 3 shows the graphs of the function  $f$  and its approximation. The latter gives a value reasonably close to  $f$  for  $\epsilon \lesssim 10^{-2}$ . Using Eqs. (50) and (52), we get the force expression in the limit  $r_{\min} \ll 4\chi/V$ :

$$F_{\text{heat}} = \frac{(\gamma - 1)GML}{\chi V^2} \left[ -1.96 - \log\left(\frac{r_{\min}V}{4\chi}\right) \right] \quad (53)$$

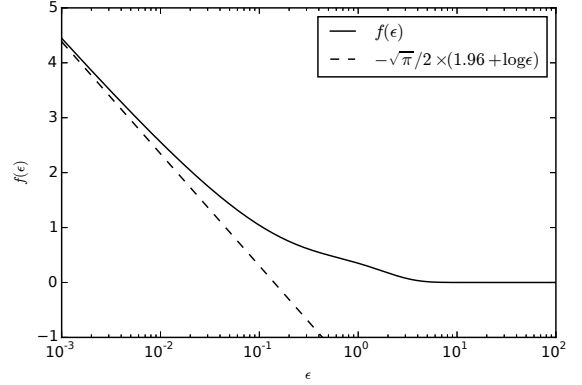


**Figure 3.** Graphs of the functions  $f$  (solid line) and its approximation given by Eq. (52).

#### 4.3 Magnitude of the minimal radius

We do not undertake here a precise calculation of the minimal radius  $r_{\min}$  to be used in Eq. (53). The heating force in the supersonic regime only weakly depends on this quantity. It corresponds to the minimal distance from the perturber at which the asymmetry in the gas density appears. It should correspond either to the body's physical size, or to the mean free path of photons (when radiative transfer is the origin of heat diffusion), whichever is larger. This last quantity is by far the largest in the application case that we will consider in section 6.

#### 4.4 Response time

The force in the supersonic case arises from the diffusion of disturbances that beat the perturber, i.e. disturbances produced at a distance  $r$  that verifies  $r^2/4\chi < r/V$ , or  $r < r_c = 4\chi/V$ . The time scale to develop the force is therefore

$$\tau' = \frac{r_c}{V} = \frac{4\chi}{V^2}. \quad (54)$$

Within a numerical coefficient, this time scale is comparable to the time scale in the subsonic regime, given by Eq. (37).

#### 4.5 Condition for linearity

We can consider that the perturbation arises from a region of size  $r_c$  next to the perturber, with a typical perturbation of density  $\Delta\rho$ , which gives rise to the force:

$$F \sim GM\Delta\rho r_c. \quad (55)$$

Equating this expression with the expression of Eq. (53) and dropping dimensionless factors of order unity, we can express the condition for linearity  $\Delta\rho \ll \rho_0$  as

$$L \ll L_c \mathcal{M}, \quad (56)$$

where  $L_c$  is defined at Eq. (35).

### 5 TOTAL FORCE ON THE PERTURBER

As said in section 2, the total force on the perturber, in the linear regime, is the sum of the standard dynamical friction

and of the heating force. When the perturber's gravity is taken into account, the flow becomes non-linear over the Bondi radius

$$R_B = \frac{GM}{c_s^2}. \quad (57)$$

Our linear analysis fails within the Bondi radius. The singular release of energy considered in section 2 should be replaced by an energy release at the Bondi radius, assumed to be small compared to the other length scales of the problem. The heat released by the planet at the centre of the Bondi sphere can diffuse outwards or can trigger acoustic waves which can redistribute the mass within the Bondi sphere. Most of the heat released at the centre by the planet will emerge of the Bondi sphere as an excess of internal energy, as required to trigger the disc's response seen in the previous sections, if the diffusion timescale over the Bondi radius is smaller than the acoustic timescale over the Bondi radius:

$$\frac{R_B^2}{4\chi} \ll \frac{R_B}{c_s}, \quad (58)$$

which can be recast as:

$$M \ll \frac{4c_s\chi}{G}. \quad (59)$$

We define the critical mass  $M_c$  as

$$M_c = \frac{c_s\chi}{G}, \quad (60)$$

and we assume in the following that the dimensionless ratio  $GM/c_s\chi = M/M_c$  is lower than one. We note that this assumption also implies that the cut-off distance  $\lambda$  is larger than the Bondi radius.

### 5.1 Regime of low Mach numbers

We specialise here to the case of low Mach numbers. In this regime, the standard dynamical friction has the expression (Ostriker 1999):

$$F_{\text{DF}} = -\frac{4\pi(GM)^2\rho_0V}{3c_s^3}, \quad (61)$$

In the work of Ostriker (1999), thermal diffusion is not considered and the gas is adiabatic. We have not analysed the standard dynamical friction in the presence of thermal diffusion. It is reasonable to assume that in the limit of a small thermal diffusion, the gas behaves adiabatically and Eq. (61) holds, whereas when thermal diffusion is large, it behaves isothermally, and the isothermal sound speed should be used in stead of the adiabatic one in Eq. (61), yielding a force larger than the adiabatic estimate by a factor  $\gamma^{3/2}$ . For the sake of definiteness we assume hereafter that the thermal diffusivity is sufficiently small that the adiabatic sound speed can be used in Eq. (61). Since the actual sound speed cannot differ from the adiabatic one by a large factor, we expect Eq. (61) to provide a correct order of magnitude of the standard dynamical friction in our case.

In order for the net force to be given by the sum of the linear estimates of the dynamical friction and heating force, the relative perturbation of the density must be small over the cut-off distance  $\lambda$  given by Eq. (24). This, along with the condition expressed by Eq. (34), requires that the Bondi radius is much smaller than  $\lambda$ , a condition that is automatically satisfied when the inequality of Eq. (59) is verified, since  $V < c$ .

### 5.2 Equilibrium speed

When the two conditions  $r_{\text{NL}}^{\text{heat}} \ll \lambda$  and  $R_B \ll \lambda$  are fulfilled, the net force is given by:

$$F = F_{\text{heat}} + F_{\text{DF}} = \frac{\gamma(\gamma-1)GML}{2\chi c_s^2} - \frac{4\pi(GM)^2\rho_0V}{3c_s^3}. \quad (62)$$

It vanishes at the equilibrium speed

$$V_0 = \frac{3\gamma(\gamma-1)Lc_s}{8\pi\rho_0GM\chi}. \quad (63)$$

This speed corresponds to a steady configuration: if the perturber is slower, it is sped up by a positive net force, and slowed down otherwise. It is noteworthy that this equilibrium speed scales with the sound speed and the luminosity to mass ratio of the perturber, and increases when the gas density or thermal diffusivity decreases. We note that the equilibrium speed is much smaller than the sound speed, as required by our hypothesis of a low Mach number, if  $L \ll L_c$ , where the critical luminosity  $L_c$  is defined at Eq. (35).

### 5.3 Regime of high Mach numbers

In an infinite homogeneous medium, the dynamical friction increases logarithmically with time, and will eventually supersede the heating force, which comes from material in the vicinity of the perturber and does not exhibit a logarithmic divergence at large scales. In a bound medium such as a slab or protoplanetary disc (Papaloizou 2002; Muto et al. 2011; Cantó et al. 2013), there is no such divergence and both the dynamical friction and heating force have similar forms, with a dimensionless factor of order unity that scales with  $|\log r_{\text{min}}|$ . Since they have same dependency on the velocity in  $V^{-2}$ , there cannot be an equilibrium speed as in the subsonic case: either the heating force is larger than the dynamical friction at all speeds, and the perturber is indefinitely accelerated, or the heating force is smaller than the dynamical friction, and the perturber is slowed down, albeit on a longer time than if dynamical friction was acting alone. This bifurcation occurs for a luminosity set by the equality of both forces (in magnitude), which yields, assuming that the logarithmic factors of the heating force and of the dynamical friction are equal:

$$L \approx \frac{4\pi}{\gamma-1}GM\chi\rho_0, \quad (64)$$

or, in terms of the critical luminosity introduced at Eq. (35)

$$L = \gamma^2 L_c \left( \frac{GM}{c_s\chi} \right). \quad (65)$$

Therefore an object that fulfils the condition of Eq. (59) by a sufficiently large amount, or that has a sufficiently large initial Mach number, can fall in the accelerated regime.

Again, we stress that standard dynamical friction has not been investigated in a gas with finite thermal diffusivity. In the supersonic regime, gas can be accreted over a region of typical size  $R_a = 2GM/V^2$  (Cantó et al. 2011). The corresponding mass flow is  $\dot{M}_{\text{gas}} = \pi R_a^2 V \rho_0$ . The energy release due to gas accretion has order of magnitude  $L_{\text{gas}} \sim GM\dot{M}_{\text{gas}}/R_a$ . When the disc has a finite thermal diffusivity, the heat thus released diffuses and gives rise to a heating force. One can check that when the perturber is subcritical, *i.e.* when Eq. (59) is satisfied, one has  $R_a \ll \lambda$ , so

that the heat release can be considered as isotropic. One can further check that the condition for linearity of Eq. (56) on the perturbation arising from  $L_{gas}$  is satisfied and that the heating force arising from  $L_{gas}$  is smaller than the standard dynamical friction. A luminosity source intrinsic to the perturber is therefore required for the heating force to overcome the standard dynamical friction.

#### 5.4 Yield

The system bears some similarities with a heat engine, as it converts part of the heat released by the perturber into work against the dynamical friction. We calculate here what fraction of the heat released goes into the work of the heating force. In the limit in which this force is much larger than the dynamical friction, it is also the yield of the conversion of the heat into macroscopic kinetic energy of the perturber. This yield reads

$$\eta = \frac{VF_{\text{heat}}}{L}, \quad (66)$$

which, in the regime of low Mach numbers, can be recast as:

$$\eta = \frac{\gamma(\gamma - 1)}{2} \left( \frac{GM}{c_s \chi} \right) \mathcal{M}, \quad (67)$$

whereas it reads, in the limit of large Mach numbers:

$$\eta = (\gamma - 1) \left( \frac{GM}{c_s \chi} \right) f \mathcal{M}^{-1}, \quad (68)$$

where  $f$  is the logarithmic factor of order unity. These expressions are in line with our constraint on the mass exposed at the beginning of section 5. They give values lower than one when the dimensionless factor  $GM/c_s \chi$  is small.

## 6 DISCUSSION

### 6.1 Disc models and assumptions

The purpose of this section is to assess whether the effect we report here could be relevant to planetary embryos or protoplanets embedded in an opaque, gaseous protoplanetary disc. Our analysis cannot be applied directly to the evaluation of the heating torque (Benitez-Llambay et al. 2015), which is a torque component that appears on planetary embryos on circular orbits when they release energy in the surrounding protoplanetary disc. The Keplerian shear of the gas is an essential ingredient of this effect, and it is neglected in the present analysis. In the same spirit, the formula of dynamical friction in a gas at rest (Ostriker 1999) cannot be used to evaluate the tidal torque exerted by the disc on a planet in circular orbit. However, it provides a useful approximation to infer the temporal behaviour of eccentricity and inclination (Papaloizou 2002; Muto et al. 2011; Rein 2012), especially when these orbital elements are large compared to the aspect ratio.

In this section we use the expression supersonic (subsonic) to refer to embryos that have an eccentricity or inclination larger (smaller) than the aspect ratio of the disc. We assume that the heating force exerted by the disc on an embryo is reasonably approximated by Eq. (53) in the supersonic case, whereas it may not necessarily be given by Eq. (30) in the subsonic case, because the Keplerian shear,

**Table 1.** Parameters from the disc model of Bitsch et al. (2015) at  $r = 3$  AU that are used in the numerical estimates of section 6. The rows represent respectively the midplane temperature, the surface density of the gas, the thermal diffusivity, the adiabatic sound speed, the midplane density, the aspect ratio of the disc, and the optical depth to the midplane  $\tau_{\text{eff}} = \kappa(\rho_0, T)\Sigma/2$ .

Parameter	Value at $t = 300$ kyrs	Value at $t = 1$ Myr
$T$ (K)	195	70
$\Sigma$ (g.cm <sup>-2</sup> )	260	190
$\chi$ (cm <sup>2</sup> .s <sup>-1</sup> )	$1.7 \cdot 10^{16}$	$9.8 \cdot 10^{14}$
$c_s$ (cm.s <sup>-1</sup> )	$10^5$	$6 \cdot 10^4$
$\rho_0$ (g.cm <sup>-3</sup> )	$4.7 \cdot 10^{-11}$	$5.8 \cdot 10^{-11}$
$h$	0.049	0.029
$\tau_{\text{eff}}$	120	47

here neglected, may be important in this case. We will work out an estimate of the eccentricity above which the shear should be unimportant in section 6.7.

The parameter space under consideration has a considerable number of dimensions. For the sake of definiteness, we consider hereafter the fiducial disc model of Bitsch et al. (2015a), corresponding to their Fig. 5, for the accretion rates  $\dot{M} = 3.5 \cdot 10^{-8} M_{\odot} \cdot \text{yr}^{-1}$  and  $\dot{M} = 8.75 \cdot 10^{-9} M_{\odot} \cdot \text{yr}^{-1}$ , which correspond respectively to the ages  $t = 300$  kyrs and  $t = 1$  Myr. In these disc models we take the conditions at  $r = 3$  AU, which is the location of the snow line at  $t = 300$  kyrs. There, there is a large drop in the temperature of the disc between these two dates, which has, as we will see, a strong impact on the different key quantities.

We consider planetary embryos or protoplanets with mass  $M$ , radius  $R$ , density  $\rho_p = 3$  g.cm<sup>-3</sup>, and a mass doubling time  $\tau_d = M/\dot{M}$ . Their luminosity is therefore:

$$L = \frac{GM^2}{R\tau_d}. \quad (69)$$

When  $\tau_d$  and  $\rho_p$  are fixed, there is a one-to-one relationship between the mass and luminosity. This allows us to translate critical luminosities into critical masses, which is likely more intuitive to most readers. For the thermal diffusivity, we use Eq. (16) of Bitsch et al. (2014), and use half the value given by the prescription of Bell & Lin (1994) to evaluate the opacity  $\kappa$  that is required in this equation (the fiducial model of Bitsch et al. has half the metallicity used by Bell & Lin). We use a ratio of specific heats  $\gamma = 1.4$ . Finally, we use the density in the midplane of the disc, which we denote  $\rho_0$ . We list our main parameters in Tab. 1.

### 6.2 Condition for linearity

We write hereafter a conservative condition for linearity on the luminosity. In the subsonic regime, we must have  $L \ll L_c/\mathcal{M}$ , whereas we must have  $L \ll L_c\mathcal{M}$  in the supersonic regime. We disregard the dependency on the Mach number, which we assume to be unity, so that we have a conservative condition on the luminosity. Translating the latter into a critical mass through the use of Eq. (69), we obtain:

$$M < \left( \frac{3}{4\pi\rho_p} \right)^{\frac{1}{5}} \left[ \frac{4\pi}{\gamma^2(\gamma - 1)} \cdot \frac{\chi^2 c_s \rho_0 \tau_d}{G} \right]^{3/5}. \quad (70)$$

For our parameters, this gives:

$$M < 6.4 \left( \frac{\tau_d}{10^5 \text{ yrs}} \right)^{3/5} M_{\oplus} \quad \text{at } t = 300 \text{ kyrs}$$

$$M < 0.18 \left( \frac{\tau_d}{10^5 \text{ yrs}} \right)^{3/5} M_{\oplus} \quad \text{at } t = 1 \text{ Myr}$$

These conditions indicate that protoplanets up to several Earth masses trigger a linear response in the disc at early time, whereas embryos slightly above Mars's size trigger a non-linear response at later times, once the disc has substantially cooled.

### 6.3 Critical mass

The critical mass given by Eq. (60) has, for our set of parameters, the following value:

$$M_c = 4.2 M_{\oplus} \quad \text{at } t = 300 \text{ kyrs}$$

$$M_c = 0.15 M_{\oplus} \quad \text{at } t = 1 \text{ Myr}$$

Its dramatic drop at larger time is essentially due to the drop in the disc's thermal diffusivity. Perturbers with a mass below the critical mass are essentially subjected to the heating force worked out in sections 3 and 4 (in a medium without shear) whereas they are necessarily subjected to a weaker force when their mass is larger than the critical mass, as shown by the considerations on the yield of section 5.4. The actual magnitude of the heating force on a perturber with a mass larger than the critical mass is nonetheless unknown at this stage. It is noteworthy that these critical masses roughly coincide with the upper values for a linear response obtained in section 6.2.

### 6.4 Response time

The velocity of an eccentric and/or inclined embryo with respect to the surrounding gas changes orientation over a dynamical time scale. This time scale must be substantially longer than the response time of the heating force, given by Eq. (37) or Eq. (54). In the supersonic regime, we can obtain a conservative estimate of the response time (*i.e.*, an upper value) by using the sound speed instead of the velocity in this equation. Conversely, the actual response time is larger than this estimate in the subsonic regime. Using this estimate, the condition for a short response time is:

$$\frac{\chi}{\gamma^2 c_s^2} \lesssim \frac{1}{\Omega}, \quad (71)$$

where  $\Omega$  is the orbital frequency. Eq. (71) can be written, dropping dimensionless factors of order unity:

$$\lambda \lesssim H, \quad (72)$$

so the condition for a short response time is equivalent to requiring a plume size smaller than the scale height  $H$  of the disc. This, in turn, can also be expressed as

$$\frac{GM_c}{c_s^2} \lesssim H, \quad (73)$$

which means that the embryos with a mass equal to the critical mass, defined at Eq. (60), must have a Bondi radius much smaller than the disc's scale height. This condition is satisfied by a very large factor for the two cases considered

in section 6.3, namely a factor of 10 in the first case, and a factor of 50 in the second one. This also suggests that even for embryos with an eccentricity as small as  $h/10 \sim 4 \cdot 10^{-3}$ , the response time of the heating force is shorter than the dynamical timescale, so that it can have an impact on the embryo's eccentricity.

An embryo travelling at a sizeable fraction of the sound speed with respect to the disc material is subjected to asymmetric heating, as more solid material impinges on its forward side. One can consider that the energy is released isotropically if the rotation period of the embryo is much shorter than the response time of the plume (strictly speaking, this is true if the rotation axis is perpendicular to the direction of motion; in the general case there is a residual anisotropy that depends on the angle between the rotation axis and the direction of motion). For our first data set (at  $t = 300$  kyrs) a conservative estimate of the response time is  $\tau \sim 8$  days, whereas it is only  $\tau \sim 1.6$  days for our second data set (at  $t = 1$  Myr). These estimates are conservative because they are evaluated using the sound speed in Eq. (37). If the embryo has a lower speed, the plume is larger and the response time longer. These typical time scales should be compared to a rotation period of  $O(10)$  hrs. The first estimate is widely larger, but the second one might be comparable to the rotational period of the slowest embryos. In this last, rare case the heating force is no longer directed along the direction of motion, but changes orientation as the embryo rotates.

### 6.5 Constraints on the cut-off distance

The heating force, in the subsonic regime, can have the expression given by Eq. (30) only if the embryo's physical radius is much smaller than the size of the heated region (the cut-off distance  $\lambda$ ). For our two data sets, this distance typically amounts to  $10^{-2}$  to  $10^{-3}$  AU, or  $10^5$  to  $10^6$  km (these values are again conservative estimates obtained using the sound speed in the expression of the cut-off distance). The plume is therefore much larger than any embedded protoplanet. Another, more demanding condition on the plume size is that it should be larger than the mean free path of photons  $(\rho_0 \kappa)^{-1} \sim H/\tau_{\text{eff}}$ , so that the evolution of the heat within the plume is governed by diffusion, as assumed in our analysis. This condition is satisfied by a factor of order 5 for our first data set ( $t = 300$  kyrs), whereas the mean free path of photons turns out to be  $\sim 3$  times larger than the conservative (minimal) plume size for our second data set ( $t = 1$  Myr). Our expression of the heating force would therefore be valid, in that second case, for embryos with Mach numbers smaller than  $1/3$ .

### 6.6 Critical luminosity in the supersonic regime

We have seen in section 5.3 that a perturber with a luminosity above the critical value given by Eq. (64) has a heating force larger than the dynamical friction at all speeds, and can be indefinitely accelerated. Above this luminosity threshold, a planetary embryo with a large eccentricity should therefore become more eccentric, rather than being circularised, since the heating force has opposite direction to the dynamical friction. Translating the luminosity threshold, through



the use of Eq. (69), into a mass threshold, we are led to:

$$M > 4\pi \left(\frac{3}{\rho_p}\right)^{\frac{1}{2}} \left(\frac{\chi\rho_0\tau_d}{\gamma-1}\right)^{\frac{3}{2}}, \quad (74)$$

which reads, for the parameters of our first data set:

$$M > 33 \left(\frac{\tau_d}{10^5 \text{ yrs}}\right)^{3/2} M_{\oplus} \quad \text{at } t = 300 \text{ kyrs}$$

The mass doubling time must be as short as 25 kyrs to get a mass threshold equal to the critical mass worked out in section 6.3. Embryos of critical mass undergoing such a vigorous accretion, if they exist, should therefore fall in the regime of indefinite acceleration.

We do not consider our second data set, since we have seen in section 6.5 that the plume size is smaller than the mean free path of photons in this case, when the Mach number exceeds 1/3.

The ultimate value of eccentricity or inclination reached in the supersonic regime is beyond the scope of this work. Additional complications arise: (i) embryos that have larger velocities with respect to the disc should have a larger accretion rate and have their luminosity increased; (ii) when the inclination becomes of the order of the disc's aspect ratio, embryos only spend a fraction of their orbit within the disc; (iii) aerodynamic drag is non-negligible for supersonic embryos up to a few Earth masses (Rein 2012); (iv) when the Mach number increases, the plume size decreases and can be comparable to the photons mean free path, in which case our expression for the heating force ceases to be valid.

### 6.7 Random velocities of embryos

We evaluate here the equilibrium speed of embryos as given by Eq. (63), and regard it as the magnitude of the random velocity with respect to their circular motion. We emphasise that this approach is not self-consistent: the equilibrium velocity exists only in the subsonic regime, for which the Keplerian shear is important, whereas it has been neglected in our analysis. Nevertheless, the Mach number that we obtain should give an indication of whether we can expect sizeable eccentricities or inclinations as an outcome of the heating force. We can evaluate the eccentricity above which the shear should be unimportant on a plume. An embryo with eccentricity  $e$ , orbital radius  $r$  and orbital frequency  $\Omega$  has relative velocity with respect to the gas  $er\Omega$ , hence a cut-off distance  $\lambda$  of order  $\chi/\gamma er\Omega$ . By requesting that this cut-off distance be smaller than its distance to corotation  $er$ , we obtain:

$$e > e_c = \sqrt{\frac{\chi}{\gamma\Omega r^2}}. \quad (75)$$

The critical value for the eccentricity in our first data set ( $t = 300$  kyrs) is  $e_c = 10^{-2}$ , whereas it is  $e_c = 3 \cdot 10^{-3}$  in our second data set ( $t = 1$  Myr). These values are significantly smaller than the aspect ratio, because the length scale of the response (*i.e.* the plume size) is much smaller than the pressure scale length. This justifies the use of the heating force expression to assess eccentricity driving even in the subsonic regime. Using Eqs. (63) and (69), we obtain

$$\frac{V_0}{c_s} = \frac{3^{2/3}\gamma(\gamma-1)M^{2/3}(4\pi\rho_p)^{1/3}}{8\pi\rho_0\chi\tau_d}. \quad (76)$$

Numerically, this gives

$$\frac{V_0}{c_s} \sim 0.2 \left(\frac{\tau_d}{10^5 \text{ yrs}}\right)^{-1} \left(\frac{M}{1 M_{\oplus}}\right)^{2/3} \quad \text{at } t = 300 \text{ kyrs}$$

$$\frac{V_0}{c_s} \sim 2.9 \left(\frac{\tau_d}{10^5 \text{ yrs}}\right)^{-1} \left(\frac{M}{1 M_{\oplus}}\right)^{2/3} \quad \text{at } t = 1 \text{ Myr}$$

These relations show that an Earth-sized planet could reach an eccentricity or inclination that represents a fair fraction of the disc's aspect ratio at  $t = 300$  kyrs. At  $t = 1$  Myr, a one Earth-mass embryo is super-critical (see section 6.3), so the relation above cannot be used for this mass. When used with the critical mass  $M = 0.15 M_{\oplus}$ , it yields a Mach number of order 0.8, larger than the threshold that we worked out in section 6.5. This nevertheless suggests that critical mass embryos (typically of Mars size) should experience a significant eccentricity or inclination excitation.

We finally compare the time scale of eccentricity driving by the heating force to the time scale of eccentricity evolution due to accretion of solids. The eccentricity of an embryo is significantly modified by accretion when the embryo has accreted a solid mass comparable to its own mass, which occurs on the mass doubling time  $\tau_d$  of the embryo. An order of magnitude of the time scale  $\tau_e$  of eccentricity excitation by the heating force can be obtained by equating the work of the heating force in the rotating frame to the energy in the epicyclic motion (the former quantity corresponds to the variation of the embryo's Hamiltonian in the frame rotating with the guiding centre's angular velocity, assumed to be constant, while the latter is the eccentricity dependent term of this Hamiltonian):

$$F_{heat} \cdot e\Omega r \cdot \tau_e \sim \frac{1}{2} M\Omega^2 (er)^2. \quad (77)$$

Using Eqs. (24), (30), (57) and (69), assuming  $e \sim h$  and neglecting dimensionless factors of order unity, we obtain:

$$\frac{\tau_e}{\tau_d} \sim \frac{\lambda R_p}{R_B^2}. \quad (78)$$

For an Earth-mass object, the first data set of Tab. 1 yields a value of 0.06 for the ratio of Eq. (78). This small value could be expected on the following grounds: the equilibrium eccentricity results from a competition between the heating force and the disc's tide. The time scale for excitation should therefore have same order of magnitude as the time scale for eccentricity damping by the disc's tide, known to be of order of a few thousand years for an Earth-mass object within a disc with parameters such as those quoted in Tab. 1 (Artymowicz 1993), whereas the mass doubling time is here  $10^5$  yrs. Similar arguments apply to the inclination excitation. The main consequence of the accretion of solids is thus by far the effect of the heating force, rather than the effect of the momentum of accreted solids.

## 7 CONCLUSION

We show that a hot body moving in an opaque, initially uniform gas is subjected to a gravitational force from the gas that differs from the standard estimate of dynamical friction, which neglects the deposition of energy in the gas by the perturber. The difference, which we call the heating force, is directed along the direction of motion, and thus opposed

to the standard dynamical friction. We give the asymptotic value of the heating force in the low and high Mach number regimes, using a linear analysis. We find it to be independent of the body’s velocity in the limit of a low Mach number. As a consequence, a motionless configuration is unstable, and the perturber is eventually pushed by the heating force along its original direction of motion, regardless of how small is its initial velocity.

The asymptotic or equilibrium velocity, when it exists, is reached when the heating force cancels the standard dynamical friction. When it does not, the heating force is larger than the standard dynamical friction at all speeds, and the perturber is indefinitely accelerated. In the limit of low Mach numbers, the equilibrium velocity scales with the luminosity to mass ratio of the perturber and with the sound speed, and is inversely proportional to the thermal diffusivity and density of the gas. From a qualitative standpoint, one could say that the perturber “surfs” on the hot trail that it creates in the gas.

Although accurate derivations of the mean eccentricity and inclination of embryos or protoplanets heated by planetesimal accretion are beyond the scope of this work, we find that the heating force should have a significant impact on the random velocities of planetary embryos embedded in opaque, gaseous discs, and with mass doubling time  $O(10^5)$  yrs. The mass range of applicability of our linear analysis depends sensitively on the disc parameters, but it is broadly in the Earth-sized range, and shifts toward lower masses as the disc cools and its thermal diffusivity decays. Clearly, the numerical estimates we present here stand only as a proof of concept, and much broader explorations of disc models and distances to the central star are necessary to evaluate the impact of the heating force in scenarios of planetary formation. This effect could potentially have an impact on the growth of oligarchs within a still optically thick gaseous disc. Standard dynamical friction has been found to play a critical role on the outcome of the giant impact phase of terrestrial planet formation. Eccentricity and inclination driving by the heating force may alter outcomes of models of super-Earths formation (Dawson et al. 2016).

A tentative explanation for the existence of chondrules is the passage of solid material through the bow shocks of eccentric planetary embryos in the solar nebula (Morris et al. 2012). Although the eccentricities required to reproduce the thermal history of chondrules are in excess of those estimated in section 6, the heating force implies more dynamically excited embryos in the presence of gas, which favours scattering, and it lengthens the damping time scale of the large eccentricities attained through scattering events.

The remaining eccentricities and inclinations after the gas disappearance depend on the time behaviour of the gas density and temperature as the gaseous disc vanishes. The thermal diffusivity of the disc is proportional to the cube of its temperature and inversely proportional to the square of its midplane density. In the last stages of the disc, when its midplane density decreases substantially but it is still large enough to be optically thick, the thermal diffusivity should increase again, shifting the domain of validity of our linear analysis back toward larger, Earth-sized objects. This could excite the eccentricity of pairs of planets brought into mean motion resonance by convergent migration, if they are still subjected to planetesimal or pebble accretion (hence hot) at

this stage. In the same spirit, this could provide the initial disc of embryos and planetesimals out of which terrestrial planets are formed with an initial angular momentum deficit (AMD, Laskar 2000), but further work is required to assess the values of the residual eccentricities and inclinations and the value of the initial AMD.

We have identified a luminosity threshold above which the heating force on a supersonic embryo should always supersede the standard dynamical friction, independently of its velocity, leading in principle to a considerable effect on eccentricity and inclination. Our numerical estimates suggest that Earth-sized bodies or below undergoing very efficient pebble accretion (Bitsch et al. 2015b) might fall into this regime.

An interesting further development would be the study of the heating force when the perturber’s velocity varies with time, as has been done for the standard dynamical friction by Namouni (2010). This would allow to quantify accurately the response time of the heating force.

Our analysis features the dimensionless ratio  $GM/c_s\chi$ . Considerations on the yield of the conversion of the energy released by the perturber into macroscopic kinetic energy suggest that the heating force should be weaker than given by our linear analysis when this ratio is larger than one. This happens when the acoustic time across the Bondi radius of the perturber becomes smaller than the diffusion time. The simulations of Benitez-Llambay et al. (2015) show that the heating torque is indeed cut off near  $3 M_\oplus$ , which corresponds precisely to the planetary mass for which these two timescales coincide.

## ACKNOWLEDGEMENTS

The authors acknowledge support from UNAM’s PAPIIT grant IN101616, as well as constructive comments from Gloria Koenigsberger, Jeffrey Fung, Pablo Benítez-Llambay, Bertram Bitsch, Wladimir Lyra and an anonymous referee.

## REFERENCES

- Artymowicz P., 1993, *ApJ*, **419**, 166  
 Bell K. R., Lin D. N. C., 1994, *ApJ*, **427**, 987  
 Benitez-Llambay P., Masset F., Koenigsberger G., Szulagyi J., 2015, *Nature*, **520**, 63  
 Bitsch B., Morbidelli A., Lega E., Crida A., 2014, *A&A*, **564**, A135  
 Bitsch B., Johansen A., Lambrechts M., Morbidelli A., 2015a, *A&A*, **575**, A28  
 Bitsch B., Lambrechts M., Johansen A., 2015b, *A&A*, **582**, A112  
 Cantó J., Raga A. C., Esquivel A., Sánchez-Salcedo F. J., 2011, *MNRAS*, **418**, 1238  
 Cantó J., Esquivel A., Sánchez-Salcedo F. J., Raga A. C., 2013, *ApJ*, **762**, 21  
 Chandrasekhar S., 1943, *ApJ*, **97**, 255  
 Dawson R. I., Lee E. J., Chiang E., 2016, *ApJ*, **822**, 54  
 Laskar J., 2000, *Physical Review Letters*, **84**, 3240  
 Morris M. A., Boley A. C., Desch S. J., Athanassiadou T., 2012, *ApJ*, **752**, 27  
 Muto T., Takeuchi T., Ida S., 2011, *ApJ*, **737**, 37  
 Namouni F., 2010, *MNRAS*, **401**, 319  
 Ostriker E. C., 1999, *ApJ*, **513**, 252  
 Papaloizou J. C. B., 2002, *A&A*, **388**, 615  
 Rein H., 2012, *MNRAS*, **422**, 3611

Rephaeli Y., Salpeter E. E., 1980, *ApJ*, **240**, 20

Sánchez-Salcedo F. J., Brandenburg A., 1999, *ApJ*, **522**, L35

This paper has been typeset from a  $\text{T}_{\text{E}}\text{X}/\text{L}^{\text{A}}\text{T}_{\text{E}}\text{X}$  file prepared by the author.